A New Technique for Shaping Axis-Symmetric Dual-Reflector Antennas Using Conic Sections

Tcharles V. B. Faria
Graduate Program in Electrical Engineering
UFMG – Av. Antônio Carlos 6627, 31270-901
Belo Horizonte, MG, Brazil
tcharlesdefaria@ufmg.br

Fernando J. S. Moreira
Dept. Electronics Engineering
UFMG – Av. Antônio Carlos, 6627, 31270-901
Belo Horizonte, MG, Brazil
fernandomoreira@ufmg.br

2019 SBMO/IEEE MTT-S International Microwave and Optoelectronics Conference (IMOC) | 978-1-7281-3099-6/20/$31.00 ©2019 IEEE | DOI: 10.1109/IMOC43827.2019.9317614

***Abstract*—This work investigates a new procedure for the shaping of axis-symmetric dual-reflector antennas to control the amplitude and phase of the aperture-field. The generatrices of sub- and main-reflectors are shaped through consecutive concatenation of conic sections. To illustrate the efficacy of the algorithm, an axis-displaced Cassegrain configuration is shaped to provide an uniform aperture illumination, under Geometrical Optics principles. The results are validated using the electromagnetic analysis provided by the method-of-moments.**

***Index Terms*—Reflector antenna shaping.**

I. Introduction

A technique for the shaping of axis-symmetric dual-reflectors antennas has been presented in [1]. The procedure is based on the concatenation of local conic sections suited to provide, according to Geometrical Optics (GO) principles, an aperture-field with uniform phase and prescribed amplitude distribution. Each set of conic sections is sequentially defined to represent the shaped reflector generatrices.

The procedure introduced in [1] presents significant advantages over traditional approaches [2], [3], as it is not necessary to solve any differential equation in the shaping process. However, the method [1] only allows the control of amplitude in the antenna aperture. For these reasons, this work presents a new formulation for the shaping of axis-symmetric dual-reflector antennas. The main aspect of the technique proposed in Section II is to represent the reflector generatrices by conic sections sequentially concatenated to each other [1], as illustrated in Fig. 1. Here we use elliptic sections to describe the main-reflector generatrix. Consequently, the shaping of the sub- and main-reflectors allows the desired illumination control at the aperture. The simultaneous control of amplitude and phase distributions aims to obtain greater viability of the radiation pattern of the shaped antennas.

II. Development of the Shaping Procedure

Each conic section S_n (with n = 1, ..., N) describing the subreflector has two foci: one is always at the origin O (feed phase-center) and another is located at point P_n. The main-reflector is generated by ellipses (M_n) consecutively

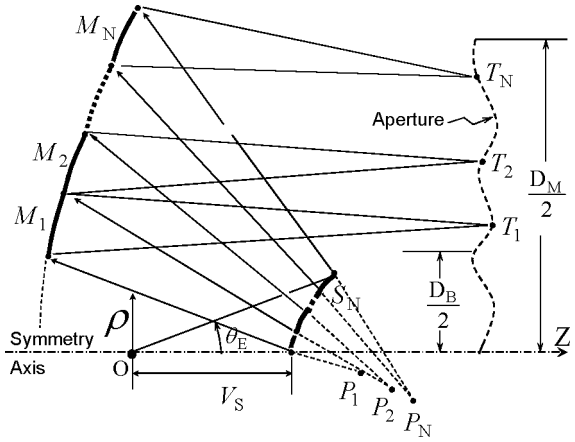

Fig. 1. Dual-reflector shaping by consecutively combining conic sections of an ADC-like configuration.

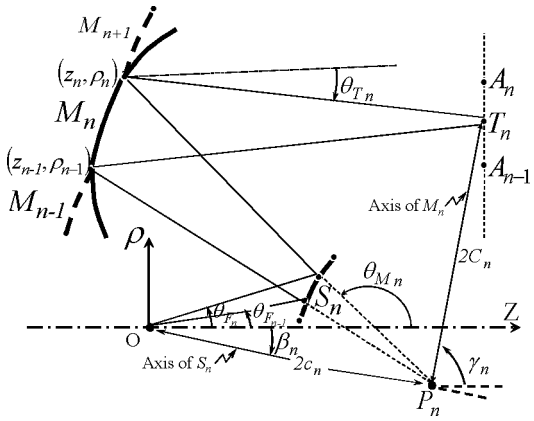

Fig. 2. Parameters of S_n and M_n.

connected. From Figs. 1 and 2, the foci of M_n are P_n and T_n (predefined at the main-reflector aperture surface).

For the ADC-like configuration shown in Fig. 1, the aperture is defined as a set of points $A_n(z_{A_n}, \rho_{A_n})$. Note that ρ_{A_n} is

978-1-7281-3099-6/19/$31.00 ©2019 IEEE

978-1-7281-3099-6/19/$31.00 ©2019 IEEE

uniformly varied from $\rho_{A_0} = D_B/2$ to $\rho_{A_N} = D_M/2$, such that $\Delta\rho_A = \rho_{A_n} - \rho_{A_{n-1}} = (D_M/2)/N$. The position of T_n is located by:

$$z_{T_n}\,\hat{z} + \rho_{T_n}\,\hat{\rho}, \tag{1}$$

where ρ_{T_n} and z_{T_n} are the coordinates of T_n. ρ_{T_n} is the midpoint between $\rho_{A_{n-1}}$ and ρ_{A_n}. In this work, we considered $z_{T_n} = z_A$, which causes an aperture-field with uniform phase and a prescribed amplitude distribution. It is emphasized that T_n can be arbitrarily localted (see Fig. 1), allowing phase control. Under GO properties, the energy contained in the ray beam (between $\theta_{F_{n-1}}$ and θ_{F_n}), incident on the conic section S_n is conserved immediately after the second reflection by the n-th ellipse (see Fig. 2). In the integral form, the conservation of energy is expressed as:

$$\int_{\theta_{F_{n-1}}}^{\theta_{F_n}} G_F(\theta_F) r_F^2 \sin\theta_F d\theta_F = L_F \int_{\rho_{A_{n-1}}}^{\rho_{A_n}} G_A(\rho)\rho d\rho, \tag{2}$$

where $G_F(\theta_F)$ is the radiated feed power density, $G_A(\rho)$ is the desired aperture (focal plane) power density and L_F is a normalization factor given by:

$$L_F = \int_0^{\theta_E} G_F(\theta_F) r_F^2 \sin\theta_F d\theta_F \Big/ \int_{D_B/2}^{D_M/2} G_A(\rho)\rho d\rho. \tag{3}$$

From (2) we get θ_{F_n} (feed ray direction) by an iterative process starting at $n = 0$ and $\theta_{F_0} = 0$ and finishing when $n = N$ for $\theta_{F_N} = \theta_E$, where θ_E is the edge angle of the subreflector.

In order to obtain each pair of S_n and M_n, for $n = 1, ..., N$, it is necessary to determine only three parameters of S_n: the interfocal distance ($2c_n$), eccentricity (e_n) and the tilt angle (β_n). Thus, three equations are required. The parameters of M_n, interfocal distance ($2C_n$), eccentricity (ϵ_n) and the tilt angle (γ_n), are further calculated from $2c_n$, e_n and β_n.

The first equation of the shaping process is obtained from the polar equation of S_n:

$$r_{F_{n-1}} = \frac{a_n}{b_n\cos\theta_{F_{n-1}} + d_n\sin\theta_{F_{n-1}} - 1}, \tag{4}$$

where

$$a_n = c_n(e_n - 1/e_n), \tag{5}$$

$$b_n = e_n\cos\beta_n, \tag{6}$$

$$d_n = e_n\sin\beta_n. \tag{7}$$

Subscript n–1 in (4) indicates that the respective values of r_F and θ_F are given from the previous iteration. The iterative process starts at $n = 0$ and $r_{F_0} = V_S$, where is the distance between the origin O and the subreflector apex, as shown in Fig. 1.

Considering the ellipse M_n, one obtains the following relation:

$$r_M(\theta_M) = \frac{A_n(\eta_M^2 + 1)}{B_n(\eta_M^2 - 1) + 2\eta_M D_n - (\eta_M^2 + 1)} \tag{8}$$

for $\theta_{M_{n-1}} \le \theta_M \le \theta_{M_n}$, where:

$$A_n = C_n(\epsilon_n - 1/\epsilon_n), \tag{9}$$

$$B_n = \epsilon_n\cos\gamma_n, \tag{10}$$

$$D_n = \epsilon_n\sin\gamma_n. \tag{11}$$

$$\eta_M = \cot\left(\frac{\theta_M}{2}\right) = \left[\frac{b_n - d_n\eta_F + 1}{d_n + \eta_F(b_n - 1)}\right], \tag{12}$$

where $\eta_F = \cot(\theta_F/2)$. In (12), it is expressed the relation between the incidence (θ_F) and reflection (θ_M) directions for the conic section S_n (see Fig. 2).

From the polar equations of S_n and M_n one can show that the length of the optical path (ℓ_n) from the feed phase-center to the focus T_n with $z_{T_n} = z_A$:

$$\ell_n = \frac{2c_n}{e_n} + \frac{2C_n}{\epsilon_n}. \tag{13}$$

Interfocal distance ($2C_n = \overline{T_nP_n}$) of (13) is obtained with aid of the Fig. 1, while ℓ_n and z_{T_n} must be specified a priori. The remaining two equations are determined by mapping the ray-direction ($\theta_F \rightarrow \theta_T$) from the feed phase-center to the focus T_n. Consequently, it can be shown that the relation between the ρ-coordinates of the main-reflector and T_n to iterations (n–1) and (n) are given by:

$$r_{M_{n-1}}(\sin\theta_{M_{n-1}} - \sin\theta_{T_{n-1}}) + \frac{2C_n}{\epsilon_n}\sin\theta_{T_{n-1}} + \rho_{P_n} = \rho_{T_n}, \tag{14}$$

$$r_{M_n}(\sin\theta_{M_n} - \sin\theta_{T_n}) + \frac{2C_n}{\epsilon_n}\sin\theta_{T_n} + \rho_{P_n} = \rho_{T_n}, \tag{15}$$

where ρ_{P_n} is the ρ-coordinate of P_n and for $\theta_{M_{n-1}} \le \theta_M \le \theta_{M_n}$ and $\theta_{T_{n-1}} \le \theta_T \le \theta_{T_n}$:

$$\sin\theta_M = \frac{2\eta_M}{\eta_M^2 + 1}; \quad \sin\theta_T = \frac{2\eta_T}{\eta_T^2 + 1}, \tag{16}$$

with η_M given by (11) and

$$\eta_T = \cot\left(\frac{\theta_T}{2}\right) = \left[\frac{g_1 - g_3 + \eta_F(1 + g_2 - g_4)}{1 - g_2 + \eta_F(g_1 + g_3) - g_4}\right], \tag{17}$$

where:

$$g_1 = D_n - d_n; \tag{18}$$

$$g_2 = B_n - b_n; \tag{19}$$

$$g_3 = d_nB_n - b_nD_n; \tag{20}$$

$$g_4 = b_nB_n + d_nD_n. \tag{21}$$

Note that γ_n is determined by Fig. 2. System (4), (14) and (15) must be solved numerically in order to obtain $2c_n$, e_n and β_n. With these parameters, $2C_n$ (Fig. 2) is readly determined and ϵ_n calculated from (13). The subreflector is given by the vector:

$$r_{F_n}(\cos\theta_{F_n}\hat{z} + \sin\theta_{F_n}\,\hat{\rho}). \tag{22}$$

with r_{F_n} given by (4) substituting (n–1) by (n). The main-reflector is located by the following vector:

$$(r_{M_n}\cos\theta_{M_n} + 2c_n\cos\beta_n)\hat{z} + (r_{M_n}\sin\theta_{M_n} + 2c_n\sin\beta_n)\hat{\rho}, \tag{23}$$

where:

$$\cos\theta_M = \frac{\eta_M^2 - 1}{\eta_M^2 + 1}. \tag{24}$$

The iterations are repeated until $\theta_{F_N} = \theta_E$ for $n = N$ [1]. The formulation introduced is derived for ADC-like antenna, but can be easily extended to three other axis-symmetric dual-reflector configurations: axis-displaced Gregorian (ADG), ellipse and hyperbola (ADH) [1].

III. Results

The synthesis process started from a classical configuration, designed with $D_M = 100\lambda$, $D_B = D_S = 10\lambda$, $\theta_E = 30°$, and $\ell_0 = 50\lambda$ (constant path length at $z_A = 0$) [1]. The operating frequency is 5 GHz, such that $D_M = 6$m. In order to evaluate the shaping procedure proposed in Section II, an ADC-like configuration is shaped with a uniform illumination distribution [$\ell_n = \ell_0$ and $G_A(\rho) =$ cte.] over the aperture ($D_B/2 \leq \rho_{A_n} \leq D_M/2$), to increase the gain of the antenna. The adopted feed model, with $p = 83$, is [1]:

$$G_F(\theta_F) = \cos^{2p}(\theta_F/2)/r_F^2. \tag{25}$$

The iterative procedure starsts with $r_{F_0} = V_S = 6.81\lambda$ for $n = 0$ and $z_{T_n} = 100\lambda$. The system of equations (4), (14) and (15) was numerically solved numerically to obtain $2c_n$, e_n and β_n. Consequently, $2C_n$, ϵ_n and γ_n were further determined.

Figure 3 showns the classical and shaped reflector's generatrices, where one can be observe the main differences between the geometries. The radiation characteristics obtained by the method-of-moments (MoM) in plane $\phi = 45°$ are represented in Fig. 4 at 5GHz. The results show good agreement when compared to a caso presented in [1] (Fig. 4). As expected, the gain of the shaped arrangment (49.2dBi) is higher than the classical configuration (47.6dBi), with an increase of the cross-polarization of the shaped antenna, according to Fig. 4. To investigate the numerical convergence of this new technique, in Fig. 5 is presented the error (RMS) as a function of the steps-numeber (N). As a reference, we use a shaped antenna with a large number of points ($\approx$ 80000) for the sub- and main-reflectors. The RMS errors were obtined from the r_{F_n} distances and z_{M_n} coordinates, respectively. From Fig. 5, it can be seen that the RMS error decreases when N increases, as expected.

IV. Conclusions

A new formulation for the GO shaping of the axis-symmetric dual-reflector antennas to control amplitude and phase of the aperture-field was presented. The procedure was easily formulated using the conic representation in polar coordinates. An ADC antenna was sucessfully shaped to obtain uniform aperture distribution [1]. The eletromagnetic perfomance of the designed antenna was achieved with accurate analysis provided by the MoM technique.

Acknowledgment

This work has been supported by the Brazillian agencies CAPES, CAPES/PROCAD 068419/14, CNPq and FAPEMIG.

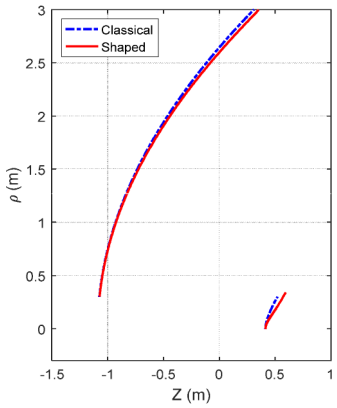

Fig. 3. Classical and shaped ADC-like configurations.

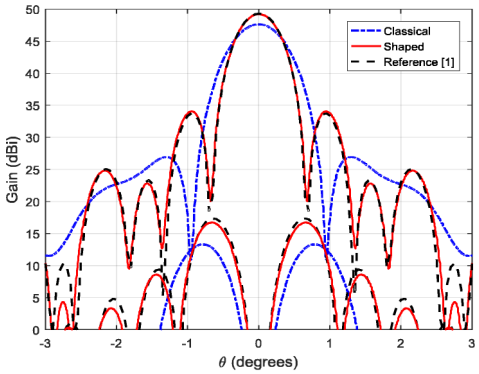

Fig. 4. MoM radiation pattern for $\phi = 45°$.

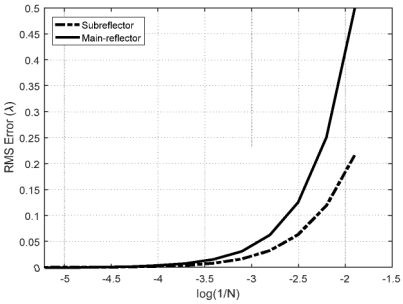

Fig. 5. RMS errors of the shaped ADC reflectors as function of N.

References

[1] F. J. S. Moreira and J. R. Bergmann, "Shaping axis-symmetric dual-reflector antennas by combining conic sections ," IEEE Trans. Antennas Propagat., vol. 59, no. 3, pp. 1042–1046, March, 2011.

[2] V. Galindo, "Design of dual-reflector antennas with arbitrary phase and amplitude distributions," IEEE Trans. Antennas Propagat., vol. AP–12, no. 4, pp. 403—408, Jul. 1964.

[3] F. J. S. Moreira, A. Prata, Jr. and J. R. Bergmann, "GO shaping of omnidirectional dual-reflector antennas for a prescribed equi-phase aperture field distribution," IEEE Trans. Antennas Propagat., vol. 55, no. 1, pp. 99–106, Jan. 2007.